The Berggren basis in elastic scattering

Fei Yuan[1, *]

[1] *National Superconducting Cyclotron Laboratory and Department of Physics and Astronomy, Michigan State University, East Lansing, MI 48824, USA*

(Dated: May 8, 2015)

We describe the theory of the Berggren basis, which unites bound, resonant, and continuum states under a single consistent framework, and demonstrate its utility by calculating the resonance in the ^{11}Be halo nucleus using a simple Woods–Saxon model. The basis is generated by applying the contour deformation method and diagonalizing the discretized Schrödinger equation in momentum space. We show that the energy obtained are comparable in accuracy to the differential equations approach, although the asymptotic behavior does not appear to be adequately described.

I. INTRODUCTION

Resonances play an important role in the understanding of many quantum systems. They are an intrinsic property of the systems and describe the energies at which cross sections are strongly enhanced.[1]

Formally, resonances appear as poles of the S-matrix in the complex momentum plane.[2] As states with complex momenta, they are not directly observable. However, if the width is sufficiently small, they can become close enough to the real momentum axis that they imprint themselves on the physical reactions, resulting in the characteristic arctangent phase shift.

Resonant states, sometimes referred to as Gamow states, are not part of the standard quantum mechanical framework due to their non-normalizability through the L^2-norm. However, with the development of the rigged Hilbert space and its associated nonhermitian formalism of quantum mechanics, the concept of resonances has been made fully rigorous.[3].

Unified with bound and continuum states under one framework through the Berggren completeness relation,[4] resonance states form a useful building block for many-body theories such as the Gamow shell model[5], the Gamow-Hartbree-Fock-Bogoliubov method,[6] and the complex coupled-cluster method.[7] All of these methods make use of the unique properties of resonant states to enable calculations of nuclei far from stability.

In this paper, we demonstrate the utility of the Berggren formalism in the calculation of a simple elastic scattering problem through the basis expansion method. We make use of the contour deformation method to construct the Berggren basis, as described in [8] and [9], in which the Schrödinger equation is analytically continued into the complex plane.

The numerical calculations are performed using a combination of Python and C code, making use of the Numpy, Scipy, and Slatec libraries. The code for this project has been made public available on GitHub.[1]

II. THEORY

A. General setup

We shall consider a simple scattering problem in which two particles interact via a spherically symmetric potential V, defined as a function of the relative coordinate $\boldsymbol{R}$. The interaction is assumed to be short-ranged and should thus become negligible after a finite radius (this excludes Coulomb interactions). The Schrödinger equation for such a system is given by:[2]

$$-\frac{1}{2\mu}\nabla^2_{\boldsymbol{R}}\psi(\boldsymbol{R}) + V(R)\psi(\boldsymbol{R}) = E\psi(\boldsymbol{R}) \tag{1}$$

where μ is the reduced mass of the system and $E = k^2/(2\mu)$ is the energy of the eigenstate.

The standard approach to solving such a problem is to use separation of variables to decompose the wave function into a sum of partial waves, each identified by orbital angular momentum ℓ and its z-projection m. Since this is a scattering problem, we may also assume azimuthal symmetry by aligning the the incident beam with the z-axis, allowing us to ignore all but the $m = 0$ partial waves:

$$\psi(\boldsymbol{R}) = \sum_{\ell=0}^{\infty} c_\ell \frac{u_\ell(R)}{R} Y_\ell^0(\hat{\boldsymbol{R}})$$

where c_ℓ are coefficients, u_ℓ is some radial wave function, and Y_ℓ^m are spherical harmonics.

B. Radial solutions

The radial wave function u_ℓ may be obtained by solving the Schrödinger-like equation:[10]

$$-\frac{1}{2\mu}\frac{\mathrm{d}^2}{\mathrm{d}R^2}u_\ell(R) + V_\ell^{\text{eff}}(R)u_\ell(R) = Eu_\ell(R) \tag{2}$$

* E-mail: yuan@nscl.msu.edu

[1] `https://github.com/xrf/phy982-proj`

[2] For clarity, we use natural units where $\hbar = 1$.

where the effective potential V_ℓ^{eff} adds an additional centrifugal term:

$$V_\ell^{\text{eff}}(R) = V(R) + \frac{\ell(\ell+1)}{2\mu R^2}$$

Equation (2) admits four different categories of solutions, known as bound, scattering, resonant, and antibound states, the choice of which depends on the boundary conditions imposed on the equation.

In bound states, the radial part $u(R)$ rapidly approaches 0 as $R \to \infty$ and are thus L^2-normalizable. Specifically, its asymptotics behave like:

$$u(R) \sim \mathrm{e}^{-\kappa R}$$

From the perspective of scattering, these may be formally treated as outgoing waves with imaginary momentum $k = \kappa\mathrm{i}$. They form a discrete spectrum of energies, all of which are negative.

In scattering states, the radial part $u(R)$ do not approach 0 and thus cannot be normalized in the usual sense. Their asymptotics behave as spherical waves:

$$u(R) \sim \mathrm{e}^{\pm \mathrm{i}kR}$$

They can be either incoming $(-)$ or outgoing $(+)$ and are characterized by positive momenta k. The states form a continuous spectrum and thus are often referred to as "continuum states", although we shall reserve the latter term for the more general set of states with complex momenta.

Resonance states have characteristics of both scattering and bound states: they form a discrete spectrum yet they are not normalizable as their asymptotics grow exponentially:

$$u(R) \sim \mathrm{e}^{(\pm k - \mathrm{i}\kappa)\mathrm{i}R}$$

The sign determines whether they are capture $(-)$ or decay $(+)$ resonances, which are analogous to incoming and outgoing waves respectively, and they affect the temporal behavior of the wave function: the former grows over time while the latter decays over time. In particular, they always occur in pairs: for every decay resonance $k - \mathrm{i}\kappa$ there is a corresponding capture resonance $-k - \mathrm{i}\kappa$. The complex energy of such a resonance state describes two essential properties of the resonance:

$$E_\mathrm{r} - \frac{\Gamma}{2}\mathrm{i} = \frac{(k - \mathrm{i}\kappa)^2}{2\mu}$$

Here, E_r is the resonance energy and Γ is the width, which quantifies the lifetime of this state. Physically relevant states – those that have a noticeable effect on cross sections – generally satisfy $\Gamma \ll E_\mathrm{r}$.

Antibound states are in a way dual to bound states. They too appear as a discrete spectrum and have imaginary momenta, but the momenta have the opposite sign and thus the wave functions grow exponentially:

$$u(R) \sim \mathrm{e}^{\kappa R}$$

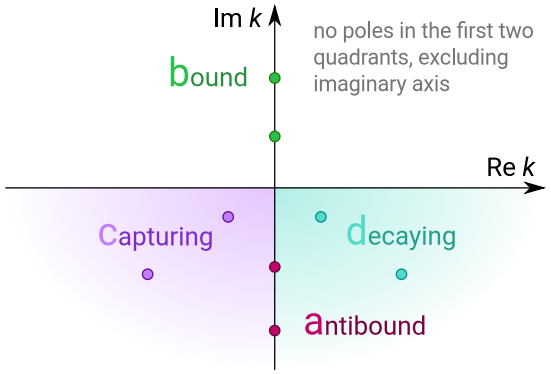

FIG. 1. Poles in the S-matrix on the complex momentum plane.

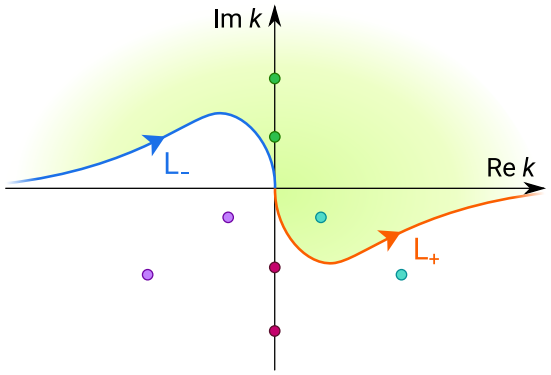

FIG. 2. A contour that may be used in the Berggren completeness relation.

Antibound states are difficult to interpret[1], although they do subtly manifest themselves in certain physical phenomena. Although we do not make use of them in this paper, the Berggren formalism can be generalized to include antibound states as well.[11]

These four kinds of states can be represented graphically as points on the complex momentum plane, as depicted in Figure 1. The bound, resonant, and antibound states appear as poles in the S-matrix, while all the points on the real axis denote scattering states.

C. Berggren basis

A well-known theorem of scattering theory states:

$$\sum_{k \in \text{bound}} |u_k\rangle\langle u_k| + \int_0^\infty |u(k)\rangle\langle u(k)|\,\mathrm{d}k = \hat{1}$$

where u_k are non-scattering wave functions (such as bound states) and $u(k)$ are the momentum space scattering wave functions. This is known as the Newton completeness relation[2] and allows bound and scattering states to be unified into one basis in which all solutions of (2) can be expanded.

However, the relation does not include resonance states. This can be remedied by choosing an alternative path for the integral, such as L_+ contour shown in 2. This leads to the Berggren completeness relation:[4]

$$\sum_{\substack{k\in\text{bound,}\\ \text{resonant}}} |u_k\rangle\langle u_k| + \int_{\mathrm{L}_+} |u(k)\rangle\langle u(k)| k^2 \,\mathrm{d}k = \hat{1} \tag{3}$$

where the sum over discrete states contains both bound and resonant states that lie above the L_+ contour. The integral over scattering states has been changed to an integral over continuum states, which have complex momenta. Such a basis, which includes resonant states in addition to bound and continuum states, is referred to as a Berggren basis.

The exponentially divergent nature of states in a Berggren basis pose a serious problem for the computation of norms and matrix elements, both of which involve integrating the states from $R = 0$ to $R = \infty$. Fortunately, there are ways to overcome the divergence using regularization techniques.

Zel'dovich proposed[12] a technique in which the integrand is multiplied by a Gaussian function $\mathrm{e}^{-\varepsilon R^2}$, which suppresses the divergence at large R. Afterwards, the $\varepsilon \to 0$ limit may be taken, hoping that a finite result is returned. The same technique was used by Berggren to prove the completeness theorem (3).

Alternatively, one may use exterior complex scaling, in which the outer part of the radial integration contour is deformed so that it approaches infinity at an angle for which the integral converges.[13]

D. Momentum-space Schrödinger equation

To solve for resonant states, it is convenient to use the momentum-space version of the Schrödinger equation. First, we define the eigenfunctions $\phi_{\boldsymbol{k}}$ of momentum $\boldsymbol{k}$, which are simply plane waves:

$$\phi_{\boldsymbol{k}}(\boldsymbol{R}) = \frac{1}{(2\pi)^{3/2}} \mathrm{e}^{\mathrm{i}\boldsymbol{k}\cdot\boldsymbol{R}}$$

The coefficient of the functions has been chosen to satisfy

$$\int_{\mathbb{R}^3} \phi^*_{\boldsymbol{k}^*}(\boldsymbol{R}) \phi_{\boldsymbol{k}'}(\boldsymbol{R}) \,\mathrm{d}^3\boldsymbol{R} = \delta(\boldsymbol{k} - \boldsymbol{k}')$$

where δ is the Dirac delta distribution. One may consider this to be a form of normalization, although this is not the standard L^2-norm.

A wave function in position space ψ may be converted into its corresponding wave function in momentum space $\tilde{\psi}$ via the Fourier transform:

$$\tilde{\psi}(\boldsymbol{k}) = \int_{\mathbb{R}^3} \phi^*_{\boldsymbol{k}^*}(\boldsymbol{R}) \psi(\boldsymbol{R}) \,\mathrm{d}^3\boldsymbol{R} \tag{4}$$

Given the symmetries of the problem, it would be useful to factor out the angular components of the transformation. To do this, we apply the plane wave expansion to $\phi_{\boldsymbol{k}}$:[14]

$$\phi_{\boldsymbol{k}}(\boldsymbol{R}) = \sum_{\ell=0}^{\infty} \sum_{m=-\ell}^{\ell} \frac{s_\ell(kR)}{kR} Y_\ell^{m*}(\hat{\boldsymbol{k}}) Y_\ell^m(\hat{\boldsymbol{R}})$$

where s_ℓ is a rescaled Riccati–Bessel function defined by

$$s_\ell(z) = \sqrt{\frac{2}{\pi}} \mathrm{i}^\ell z j_\ell(z)$$

and j_ℓ is the spherical Bessel function of order ℓ. Physically, $s_\ell(kR)$ are partial wave scattering states of (2) when the interaction V is absent. Substituting the expansion into (4) and assuming azimuthal symmetry gives:[3]

$$\tilde{\psi}(\boldsymbol{k}) = \sum_{\ell=0}^{\infty} c_\ell \frac{\tilde{u}_\ell(k)}{k} Y_\ell^0(\hat{\boldsymbol{k}})$$

where

$$\tilde{u}_\ell(k) = \int_0^\infty s^*_\ell(k^*R) u_\ell(R) \,\mathrm{d}R$$

is the momentum-space analog of u_ℓ. The position-space wave function can also be recovered from $\tilde{u}_\ell(k)$ by performing the inverse transform:

$$u_\ell(k) = \int_0^\infty s_\ell(kR) \tilde{u}_\ell(k) \,\mathrm{d}k$$

Similarly, an interaction in position space U can be transformed into its momentum-space version $\tilde{U}$ via a Fourier-like transform:

$$\tilde{U}(\boldsymbol{k}, \boldsymbol{k}') = \int_{\mathbb{R}^3} \phi^*_{\boldsymbol{k}^*}(\boldsymbol{R}) U(\boldsymbol{R}) \phi_{\boldsymbol{k}}(\boldsymbol{R}) \,\mathrm{d}^3\boldsymbol{R}$$

For a spherically symmetric interaction, that is, $U(\boldsymbol{R}) = V(R)$, the plane wave expansion can be used to factor out the angular components in the same manner:

$$\tilde{U}(\boldsymbol{k}, \boldsymbol{k}') = \sum_{\ell=0}^{\infty} \sum_{m=-\ell}^{\ell} Y_\ell^m(\hat{\boldsymbol{k}}) \frac{\tilde{V}_\ell(k, k')}{kk'} Y_\ell^{m*}(\hat{\boldsymbol{k}}')$$

where

$$\tilde{V}_\ell(k, k') = \int_0^\infty s^*_\ell(k^*R) V(r) s_\ell(k'R) \,\mathrm{d}R \tag{5}$$

In practical calculations, the integral (5) is usually performed up to a certain cut-off $R_{\max}$.

---

[3] In the original presentation, we used a different definition of the momentum wave function φ_ℓ, which is related to the current definition via $\varphi_\ell(k) = \tilde{u}_\ell(k)/k$.

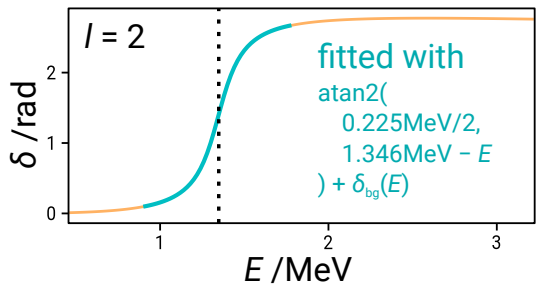

FIG. 3. Fitting the energy dependence of the phase shift with $\mathrm{atan2}(\Gamma/2, E_\mathrm{r} - E)$ to obtain the resonance parameters.

To obtain the momentum-space equation, we apply the Fourier transform in (4) to equation (1):

$$\frac{1}{2\mu}k^2\tilde{\psi}(\boldsymbol{k}) + \int_{\mathbb{R}^3}\tilde{U}(\boldsymbol{k},\boldsymbol{k}')\tilde{\psi}(\boldsymbol{k}')\,\mathrm{d}^3k' = E\tilde{\psi}(\boldsymbol{k})$$

We then make use of the previous results to derive the Schrödinger equation in momentum space for each partial wave in a spherically symmetric potential:

$$\frac{1}{2\mu}k^2\tilde{u}_\ell(k) + \int_0^\infty \tilde{V}_\ell(k,k')\tilde{u}_\ell(k')\,\mathrm{d}k' = E\tilde{u}_\ell(k) \qquad (6)$$

III. IMPLEMENTATION

A. The ^{11}Be system

We shall consider the ^{11}Be halo nucleus, which may be modeled by a valence neutron on top of an inert ^{10}Be core (mass number $A = 10$). The interaction between the bodies is described by a simple Woods–Saxon potential

$$V(R) = \frac{V_0}{1 + \mathrm{e}^{(R-R_\mathrm{ws})/a_\mathrm{ws}}}$$

where the radius $R_\mathrm{ws} = 1.2A^{1/3}\,\mathrm{fm}$, the diffuseness $a_\mathrm{ws} = 0.65\,\mathrm{fm}$, and depth $V_0 = -61.1\,\mathrm{MeV}$. The reduced mass of this system is $\mu = \frac{1}{2} \times 0.0478450\,\mathrm{MeV}^{-1}\,\mathrm{fm}^{-2}$.

B. Contour deformation

To obtain a Berggren basis with complex momenta, the integration contour of (6) must deformed to some new contour L_+ so as to enclose at least one resonant state:

$$\frac{1}{2\mu}k^2\tilde{u}_\ell(k) + \int_{\mathrm{L}_+} \tilde{V}_\ell(k,k')\tilde{u}_\ell(k')\,\mathrm{d}k' = E\tilde{u}_\ell(k) \qquad (7)$$

This requires some *a priori* knowledge of where the state is likely to be found.

Fortunately, we have previously solved the ^{11}Be system using the standard approach of applying a differential equation solver and matching the asymptotic boundary conditions to obtain the partial wave S-matrix elements and phase shifts. From this calculation, a resonance of energy $E_\mathrm{r} = 1.346\,\mathrm{MeV}$ and width $\Gamma = 0.225\,\mathrm{MeV}$ was found for the $\ell = 2$ partial wave, as shown in Figure 3. We thus expect to find a resonant state with the same parameters.

The contour we choose shall be a simple piecewise-linear contour from k_0 to k_a to k_b to k_max. The initial k_0 is a positive value close to zero, but not exactly zero to avoid divergences in the evaluation of the spherical Bessel function. The point k_a is chosen to lie somewhere in the fourth quadrant, deforming the contour so as to enclose the resonant state. The point k_b lies on the real axis, bringing the contour back. Finally, the point k_max, still on the real axis, ends the contour and is thus the maximum momentum contained within the basis. Ideally, k_max should be as large as is necessary to obtain an acceptable result.

C. Discretization of the contour

To perform the calculation numerically, the integral in (7) must be converted into a discrete sum. There are many ways in which this can be done. We shall use the quadrature technique, which allows analytic integrals to be approximated well with a finite, carefully chosen set of points ("nodes") κ and weights w_κ:

$$\int_{L_+} \tilde{V}_\ell(k,k')\tilde{u}_\ell(k')\,\mathrm{d}k' \approx \sum_{\kappa\in\mathrm{L}_+} \tilde{V}_\ell(k,\kappa)\tilde{u}_\ell(\kappa)w_\kappa$$

Since contour is defined in terms of three linear pieces, we shall apply the quadrature rule to each of the three segments separately. The quadrature scheme that we use is the standard Gauss–Legendre quadrature scheme, good for smooth polynomial-like functions.

After discretization, the equation (7) takes on the following form:

$$\frac{1}{2\mu}k^2\tilde{u}^\ell_k + \sum_{\kappa\in\mathrm{L}_+} \tilde{V}^\ell_{k\kappa}\tilde{u}^\ell_\kappa w_\kappa = E\tilde{u}^\ell_k$$

which can be solved as an eigenvalue problem

$$\sum_{\kappa\in\mathrm{L}_+} \tilde{H}^\ell_{k\kappa}\tilde{u}^\ell_\kappa = E\tilde{u}^\ell_k$$

with a Hamiltonian matrix

$$\tilde{H}^\ell_{k\kappa} = \frac{1}{2\mu}k^2\delta_{k\kappa} + \tilde{V}^\ell_{k\kappa}w_\kappa$$

Note that the Hamiltonian matrix is not hermitian, which prevents the use of the efficient hermitian algorithms. Despite this, the matrix can still be rewritten into a complex-symmetric form, which may allow for some optimizations.[15]

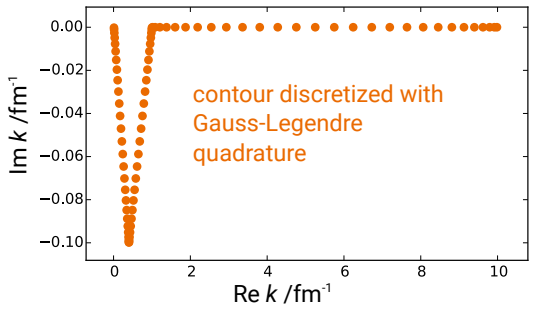

FIG. 4. A discretized Gauss-Legendre contour with 80 points.

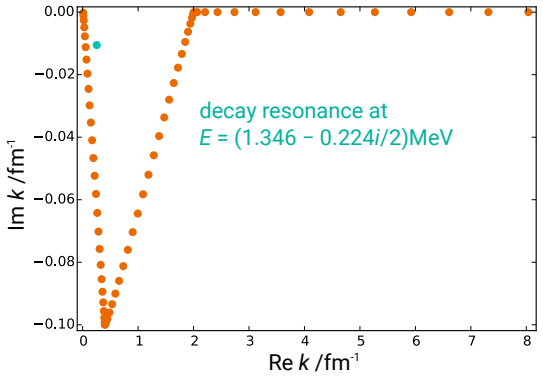

FIG. 5. Momenta of the Berggren basis states for the $\ell = 2$ partial wave.

IV. RESULTS

A. Resonant state

Figure 4 shows the typical discretized contour that is used in our calculations. The points are not evenly spaced; in particular, the points are denser near the endpoints, which is typical for Gauss-Legendre quadrature.

The contour is chosen specifically to enclose the expected resonance at $E_\mathrm{r} = 1.346\,\mathrm{MeV}$ for the $\ell = 2$ partial wave, whose complex momentum is approximately $(0.254 - 0.011\mathrm{i})\mathrm{fm}^{-1}$.

After diagonalization, the energy eigenvalues are plotted in Figure 5. The majority of the points line on the original contour: these are the continuum states in the Berggren basis. However, there is one state that lies outside the contour, indicating that it is likely a resonant state. The position-space wave function of this resonant state, plotted in Figure 6, is remarkably similar to a bound state like behavior when R is small.

The complex momentum of this resonant state is $(0.254 - 0.011\mathrm{i})\mathrm{fm}^{-1}$ and its complex energy is $(1.346 - 0.224\mathrm{i}/2)\mathrm{MeV}$, both of which are in agreement with the previous results, albeit with a slight discrepancy in the width of around 0.001 MeV. This could be attributed to either uncertainties in the previous result, perhaps due to a fitting error, or those in the current result.

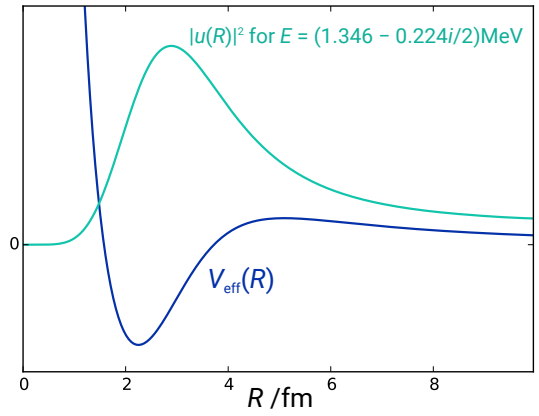

FIG. 6. Resonant state for the $\ell = 2$ partial wave.

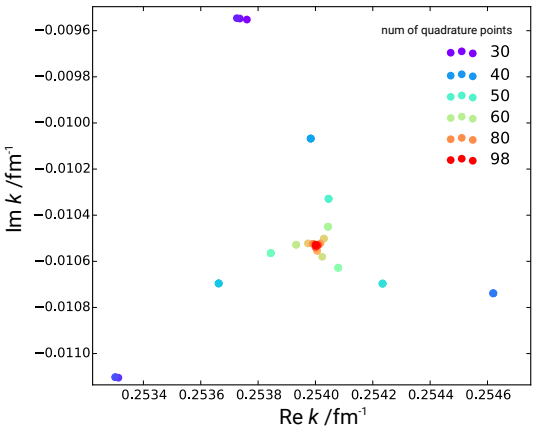

FIG. 7. Convergence of the resonant state with respect to the number of points in the discretized contour. The legend has been trimmed down for clarity, but there are in fact many more colors in this plot than are shown in the legend.

B. Convergence

To understand the uncertainty of our results, we must consider the various potential sources of error. It is possible that there may be insufficient points in the discretization of the contour, leading to a poor result. We thus varied the number of discretization points and plotted the behavior of the resonant momentum, shown in Figure 7. All other parameters were kept constant for consistency. The plot shows a clear trend towards convergence, and by around 80 points the uncertainty is already well within $10^{-4}\,\mathrm{fm}^{-1}$. There is some peculiar behavior, however. Firstly, there is a noticeable amount of clusterization of the points for adjacent numbers of quadrature points, thus the convergence appears to occur in large discrete steps. Secondly, there is an emergent triangular pattern in the plot, which indicates that there is some sort of approximate 3-fold symmetry, perhaps an artifact of the contour's shape. For future investigations, it would be useful to use a completely different contour and observe

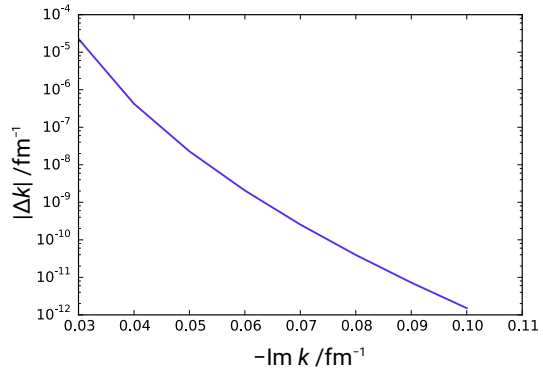

FIG. 8. Convergence of the resonant state with respect to the location of k_a.

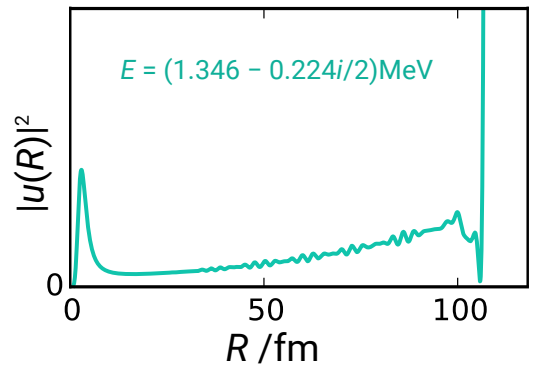

FIG. 9. Poor asymptotics of the resonant state for the $\ell = 2$ partial wave, as indicated by the small oscillations as well as the sudden cliff at around 100 fm. The correct behavior is a steady exponential growth.

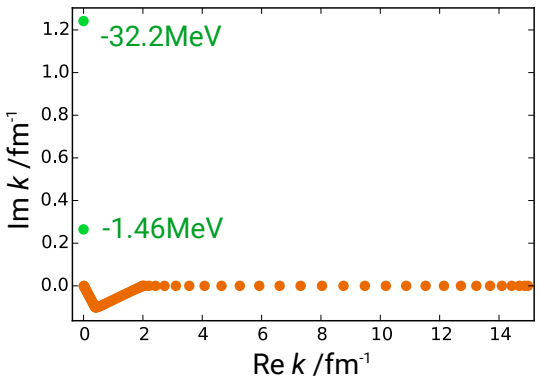

FIG. 10. Momenta of the basis states for the $\ell = 0$ partial wave.

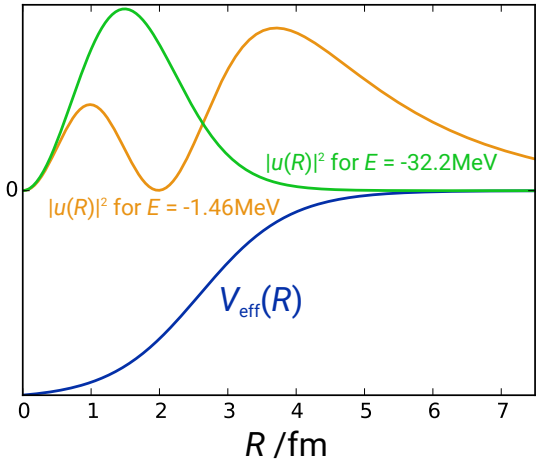

FIG. 11. Bound states for the $\ell = 0$ partial wave.

whether this pattern persists.

Another potential source of error is in the shape of the contour. Consider, for example, the location of k_a. To investigate this, we gradually increased the imaginary component of k_a from $0.02\,\mathrm{fm}^{-1}$ to $0.10\,\mathrm{fm}^{-1}$ in steps of $0.01\,\mathrm{fm}^{-1}$ and recorded how far the resonant momentum has shift between each step of k_a. This is plotted in Figure 8. The result shows an exponential decrease in the shift, suggesting that convergence is very rapid. Eventually, the shift reaches saturation once it becomes as small as the floating-point precision (not shown in the figure).

The choice of $k_{\max}$, similar to k_a, appears to make very little difference beyond a certain point. We found that $k_{\max} \geq 3\,\mathrm{fm}^{-1}$ appears to be more than sufficient. We also found the results to be largely insensitive of k_b – the resonant momentum fluctuations were below $10^{-9}\,\mathrm{fm}^{-1}$.

The radius cut-off, $R_{\max}$ is also one of the adjustable parameters. Similar to $k_{\max}$, a minimum of 30 fm appeared to be sufficient to ensure convergence.

We remark that despite the accurate momenta, the asymptotics of the position-space wave functions are quite dubious: they can fluctuate significantly depending on the parameters. The method is able to compute the position-space wave functions accurately for small radii, but as the radius increases the accuracy decreases rapidly, as shown in Figure 9. This is alleviated somewhat by increasing the number of discretization points, but it can quickly become very costly. This is quite unlike the differential equation approach that we had previously used where the asymptotics are nearly exact. It may be possible to remedy this by matching the boundary at some finite radius with the exact theoretical result.

C. Bound states

Interestingly, although not surprisingly, the same method works not only for computing resonant states but also bound states. We applied the same technique as before to the $\ell = 0$ partial wave and were able to resolve two bound states with energies $-32.2\,\mathrm{MeV}$ and $-1.46\,\mathrm{MeV}$ as shown in Figure 10. The choice of the contour did not matter, since bound states are always included in the basis, but we kept our original contour for consistency. The position-space wave functions of the bound states are plotted in Figure 11.

V. CONCLUSIONS

We have performed a calculation of the ^{11}Be system using a simple model and have extracted a resonant state with characteristics consistent with our previous calculation through an entirely different approach. In doing so, we have demonstrated a technique for calculating resonant states using a basis expansion approach, showing both its utility and robustness.

For future investigations, there are several directions in which the project can continue. For one, it would be useful to further analyze the uncertainities in the calculations due to other factors, such as the choice of the quadrature method, the location of k_0, or the specified tolerance in the calculation of $\tilde{V}$ matrix elements.

Another potential direction would be to incorporate more complicated interactions, such surface Woods–Saxon potentials, or spin-orbit potentials.

It would be interesting to see how far the technique can be generalized. One could look into situations where the spherical symmetry is lost. One could also incorporate the long-ranged Coulomb potential into the Berggren basis. There are some major complications that arise in this, for both theoretical and numerical reasons. For example, calculation of complex Coulomb wave functions is not nearly as straightforward as calculating complex Bessel functions. The proof of the completeness relation for Coulombic potential is also much more complicated than that of short-ranged potentials.[16]

ACKNOWLEDGMENTS

This work was developed as a project for the PHY982 Nuclear Dynamics course. We wish to thank the professors for their lectures and guidance throughout the course. Although it was brief due to the half-semester schedule, the course was nonetheless helpful in broadening our knowledge in nuclear theory as well as gaining a firmer understanding of scattering theory.

[1] N. Michel, W. Nazarewicz, M. Płoszajczak, and T. Vertse, Journal of Physics G: Nuclear and Particle Physics **36**, 013101 (2009).
[2] R. G. Newton, *Scattering Theory of Waves and Particles* (McGraw-Hill Book Company, United States of America, 1966).
[3] A. Böhm and J. D. Dollard, *The Rigged Hilbert Space and Quantum Mechanics*, Vol. 78 (Springer Berlin Heidelberg, 1978).
[4] T. Berggren, Nuclear Physics A **109**, 265 (1968).
[5] G. Hagen, M. Hjorth-Jensen, and N. Michel, Phys. Rev. C **73**, 064307 (2006).
[6] N. Michel, K. Matsuyanagi, and M. Stoitsov, Phys. Rev. C **78**, 044319 (2008).
[7] G. Hagen, D. Dean, M. Hjorth-Jensen, and T. Papenbrock, Physics Letters B **656**, 169 (2007).
[8] G. Hagen, *The Contour Deformation Method in Momentum Space, and Effective Interactions for Weakly Bound Nuclei*, Ph.D. thesis, University of Bergen (2005).
[9] J. Bengtsson, P. Granström, O. Embréus, V. Ericsson, and N. Wireklint, "Quantum resonances in a complex-momentum basis," B.S. thesis (2013), Chalmers University of Technology, `http://publications.lib.chalmers.se/records/fulltext/179709/179709.pdf`.
[10] I. J. Thompson and F. M. Nunes, *Nuclear Reactions for Astrophysics: Principles, Calculation and Applications of Low-Energy Reactions* (Cambridge University Press, New York, United States of America, 2009).
[11] T. Vertse, P. Curutchet, R. Liotta, and J. Bang, Acta Physica Hungarica **65**, 305 (1989).
[12] Y. B. Zel'dovich, JETP (Soviet Physics) **39**, 776 (1960).
[13] B. Gyarmati and T. Vertse, Nuclear Physics A **160**, 523 (1971).
[14] R. Mehrem, Applied Mathematics and Computation **217**, 5360 (2011).
[15] I. Bar-On and M. Paprzycki, Numerical Algorithms **18**, 195 (1998).
[16] N. Michel, Phys. Rev. C **83**, 034325 (2011).